https://doi.org/10.2352/issn.2169-2629.2020.28.55

Digital camera-based spectral estimation in open environment based on imaging condition correction

Jinxing Liang[1], Kaida Xiao[2]
[1]College of Mathematics and Computer Science, Wuhan Textile University, Wuhan, Hubei, China
[2]School of Design, University of Leeds, Leeds, United Kingdom

Abstract

Digital camera-based spectral estimation in open environment is a challenge in current stage. Although some methods have been proposed in recent years, the methods do not consider the exposure inconsistency between camera spectral characterization and spectral estimation applications, that makes the proposed method cannot for practical applications. We proposed here a spectral estimation method based on imaging condition correction of which can deal with the problem exist in current methods. Using the whiteboard and raw camera response, the imaging conditions of open environment is recorded and corrected to the reference imaging conditions, and the surface spectral of object is estimated using the established spectral estimation matrix in the reference imaging conditions. The proposed method in three application models are tested and compared. The result shows that the adaptive model for imaging condition correction gives the best spectral estimation accuracy.

Introduction

The surface spectral of object plays an important role in the fields such as color science, computer vision, biomedical, cultural relics protection and so on [1-4]. Spectral measurement is the foundation of its application, the traditional spectral measurement equipment such as spectrophotometer and spectral camera can realize the accurate measurement of spectral. Digital camera-based spectral estimation for spectral measurement is a different technique proposed in recent years [4]. Although its measurement accuracy is hard to compete with the traditional measurement equipment, it can overcome the application limitation of spectrophotometer based on single point, and overcome application limitations of the spectral camera such as poor geometric accuracy, low spatial resolution and poor system flexibility. In addition, the low price of the equipment, the flexible application of the system, and the easy-to-transform of its technology in smart-phones are also some of its advantages, the digital camera-based spectral estimation has become a valuable research direction in recent years[1-7,12].

Digital camera-based spectral estimation need training set to construct the spectral estimation matrix in specific imaging condition (which is called camera spectral characterization), and the surface spectral of object is then estimated using the established estimation matrix under the same imaging conditions. Nowadays, digital camera-based spectral estimation has made great achievements in the laboratory, and many superior methods have been proposed for spectral estimation, however, without the color chart as portable training set, how to use digital camera-based spectral estimation in open environment (such as outdoor and indoor unknown illumination environment) is a challenge in current stage. Some researches have been carried out for the digital camera-based spectral estimation in open environment, Shrestha and Hardeberg proposed a approach for multispectral imaging based on the dual-RGB camera system [8], Khan *et al*. proposed the multispectral imaging method based on spectral adaptation transform [9], and Zhang *et al*. proposed the digital camera-based spectral estimation method via white balance and link function [10]. Although the methods can realize the application of the system in open environment theoretically, they neglected the influence of the exposure level (determined by imaging parameters of camera and illuminance of the light source) on the spectral estimation. If the exposure level is inconsistency between camera spectral characterization and spectra estimation applications, it will cause unpredictable error to spectral estimation, especially when the nonlinear camera response expansion (e.g. the polynomial-based camera response expansion) is used in spectral estimation. According the research outcome of Finlayson *et al*., the nonlinear camera response expansion will cause inevitable color correction error when the exposure is inconsistency between camera color characterization and color correction applications [11], the problem is also exist in digital camera-based spectral estimation.

With consideration of the problems exist in current methods, we proposed a digital camera-based spectral estimation method in open environment based on imaging condition correction. The imaging conditions is recorded and corrected using whiteboard and the linear raw camera response. Details of the proposed method is introduced in section 2, experiment and discussion of the method are described in section 3 and section 4, and the research is summarized in the last section.

Model and Method

System model

In this work, we suppose a ideal simplified linear camera imaging model without consideration of the imaging noise. In such a model, the camera response formed in a pixel of an image can be formulated as equation (1) ,

$$d_i = \int_{\Omega} l(\lambda) s_i(\lambda) r(\lambda) d\lambda \quad (1)$$

where the camera response d_i is related to the channel i of a pixel in the image, λ is the wavelength, $l(\lambda)$ is the relative spectral radiance of the illuminant, $s_i(\lambda)$ is the spectral sensitivity function of the ith channel of the camera, $r(\lambda)$ is the spectral reflectance of a pixel in the image, Ω is the spectral integrated range of the camera imaging system. In practice, we can formulate a discrete version of equation (1) as:

$$\mathbf{d} = \mathbf{Mr} \quad (2)$$

where $\mathbf{d}$ is the response vector of a pixel in the image, $\mathbf{M}$ is the overall spectral sensitivity function matrix of the camera imaging system including the product of the matrix form of $l(\lambda)$ and $s_i(\lambda)$, $\mathbf{r}$ denotes the spectral reflectance vector of a pixel. For digital camera-based spectral estimation, the first step is to construct the spectral estimation matrix based on the camera imaging model. Many methods have been proposed to calculate the spectra estimation matrix, such as pseudoinverse, PCA, Wiener estimation method and so on [12]. The commonly used pseudoinverse method that also adopted in this study is shown as equation (3),

$$\mathbf{Q} = \mathbf{R}_{\text{train}}\mathbf{D}_{\text{train}}^{+} \tag{3}$$

where $\mathbf{Q}$ is the spectral estimation matrix, $\mathbf{R}_{\text{train}}$ and $\mathbf{D}_{\text{train}}$ are the spectral and camera response matrix of training set, and superscript + is the pseudoinverse operator. With the established spectral estimation matrix $\mathbf{Q}$, the spectral reflectance of any pixel in the image can be estimated as shown in equation (4),

$$\mathbf{r}_{\text{test}} = \mathbf{Q}\mathbf{d}_{\text{test}} \tag{4}$$

where $\mathbf{d}_{\text{test}}$ is the camera response vector of a pixel, $\mathbf{r}_{\text{test}}$ is the corresponding estimated spectral reflectance vector. The current researches of digital camera-based spectral estimation are all based on the above system model, and it is the same for this study.

Proposed method

Based on the system model described above, we proposed a method of digital camera-based spectral estimation in open environment based on imaging condition correction. The details of the method are as follows.

First, under the reference imaging conditions (usually in the laboratory with known illuminant), the spectral estimation matrix is established using training set, as shown in equation (3). Especially, to avoid the exposure variability of the established spectral estimation matrix $\mathbf{Q}$, the proposed root polynomial-based camera response expansion by Finlayson *et al.* [11] is introduced in the proposed method. For example, the 3rd degree root polynomial-based camera response expansion with 13 items is illustrated in equation (5),

$$\mathbf{d}_{\text{exp}} = [r\, g\, b\ \sqrt{rg}\ \sqrt{rb}\ \sqrt{gb}\ {}^{1/3}\!\sqrt{r^2 g}\ {}^{1/3}\!\sqrt{r^2 b}\ \ldots \\ {}^{1/3}\!\sqrt{g^2 r}\ {}^{1/3}\!\sqrt{g^2 b}\ {}^{1/3}\!\sqrt{b^2 r}\ {}^{1/3}\!\sqrt{b^2 g}\ {}^{1/3}\!\sqrt{rgb}]^T \tag{5}$$

where r, g and b are the camera response of R-, G- and B-channel, respectively, $\mathbf{d}_{\text{exp}}$ is the expanded camera response vector. Furthermore, the raw camera response of whiteboard $\mathbf{d}_{\text{white,ref}}$ is acquired for subsequent imaging condition correction.

Second, the raw camera response of the measurement object $\mathbf{d}_{\text{obj}}$ is captured and acquired in open environment. And similarly, the raw camera response of whiteboard $\mathbf{d}_{\text{white,open}}$ in open environment is also acquired for the imaging condition correction purpose.

Third, the imaging conditions of the object camera response is corrected to the reference imaging conditions. Theoretically, there are three application models in the proposed method for imaging condition correction, and the details of the three models are as follows.

Model-1*: The incomplete imaging condition correction model*. The incomplete imaging condition correction model is the simplest way for imaging condition correction in the proposed method, where a diagonal matrix $\mathbf{M}_1$ is constructed based on the raw camera response of whiteboard. The method to construct $\mathbf{M}_1$ is shown in equation (6),

$$\mathbf{M}_1 = \text{diag}(\mathbf{d}_{\text{white,ref}} \cdot / \mathbf{d}_{\text{white,open}}) \tag{6}$$

where $\mathbf{d}_{\text{white,ref}}$ and $\mathbf{d}_{\text{white,open}}$ are the raw camera response of whiteboard in reference imaging conditions and in open environment respectively, the symbol ./ represent the element division operator, the diag($\cdot$) is the diagonal function, and $\mathbf{M}_1$ is the incomplete imaging condition correction matrix. With the constructed matrix $\mathbf{M}_1$, the imaging conditions of the object camera response can be corrected as indicated in equation (7), where $\mathbf{d}_{\text{obj,corr}}$ is the corrected object camera response.

$$\mathbf{d}_{\text{obj,corr}} = \mathbf{M}_1\mathbf{d}_{\text{obj}} \tag{7}$$

Model-2*: Imaging condition correction using the unified color correction matrix*. Influenced by the overlapping of sensitivity functions between camera channels [9,13], the imaging condition correction matrix $\mathbf{M}_1$ cannot be used to completely correct the color error caused by the difference of illuminant between camera spectral characterization and spectral estimation applications. Therefore, the further color correction of the object camera response is necessary to improve the spectral estimation accuracy. In this model, similar to the research of Khan *et al.* [9], we suppose the illuminant in open environment is unknown but belongs to one of the commonly used illuminants, and a unified color correction is helpful to correct the color bias caused by the difference of illuminant. Therefore, we use the similar method as Khan *et at.* to calculate a unified color correction matrix for further color correction applications.

*Step*1: Based on the ideal camera imaging model illustrated in equation (1), the camera response of training set is calculated under some commonly used illuminants and under the reference illuminant. And the exposure is set to same between each of the commonly used illuminant and the reference illuminant.

*Step*2: The unified color correction matrix $\mathbf{M}_{\text{u}}$ is calculated as shown in equation (8), where $\mathbf{D}_{\text{train},i}$ is the raw camera response of training set under the ith common illuminant, $\mathbf{D}_{\text{train,ref}}$ is the raw camera response of training set under the reference illuminant, symbol \ represent the least square operator, and n is the number of the commonly used illuminants.

$$\mathbf{M}_{\text{u}} = \begin{bmatrix} \mathbf{D}_{\text{train},1} \\ \mathbf{D}_{\text{train},2} \\ \vdots \\ \mathbf{D}_{\text{train},i} \end{bmatrix} \Bigg\backslash \begin{bmatrix} \mathbf{D}_{\text{train,ref}} \\ \mathbf{D}_{\text{train,ref}} \\ \vdots \\ \mathbf{D}_{\text{train,ref}} \end{bmatrix}, (i = 1, 2, \cdots, n) \tag{8}$$

With the matrix $\mathbf{M}_{\text{u}}$, the imaging conditions of the object raw camera response is corrected as indicated in equation (9).

$$\mathbf{d}_{\text{obj,corr}} = \mathbf{M}_1\mathbf{M}_{\text{u}}\mathbf{d}_{\text{obj}} \tag{9}$$

Model-3*: Imaging condition correction using the adaptive color correction matrix*. Different from the unified imaging condition correction matrix, in this model, we suppose the illuminant of the open environment can be estimated based on whiteboard and a illuminant database, and some equivalent illuminants can be selected from the illuminant database. Therefore, the adaptive color correction matrix can be constructed for further color correction applications.

*Step*1: The simulation raw camera response of whiteboard is calculated under each of the illuminant in database.

*Step*2: Both the simulation raw camera response and the raw camera response of whiteboard under reference illuminant are normalized to the maximum.

*Step*3: Based on the normalized raw camera response of whiteboard, the angle error (*AE*) and euclidean distance (*ED*) between each of the candidate illuminants and the reference illuminant is calculated. And the total error (*TE*) is further calculated based on *AE* and *ED* as shown in equation (10), where norm($\cdot$) is the maximum normalization function.

$$TE = \text{norm}(AE) \cdot \text{norm}(ED) \tag{10}$$

*Step*4: The first k illuminants with the relative small total error (*TE*) are selected as the equivalent illuminants, and the adaptive color correction matrix $\mathbf{M}_{\text{a}}$ is calculated as same to the unified color correction matrix described above. With the matrix $\mathbf{M}_{\text{a}}$, the imaging conditions of the object camera response is corrected as shown in equation (11).

$$\mathbf{d}_{\text{obj,corr}} = \mathbf{M}_1\mathbf{M}_{\text{a}}\mathbf{d}_{\text{obj}} \tag{11}$$

Finally, the surface spectral of the object is estimated using the established spectral estimation matrix **Q** in the reference imaging condition. It should be noted that the corrected object raw camera response should perform the same degree of root polynomial expansion as did the training sample set.

Experimental

The proposed method in above three models are tested in this section. The simulation imaging system is established using the camera sensitivity function of Nikon D5100 [14]. The white patch of No.E5 in X-rite ColorChecker SG chart is used as the whiteboard for imaging condition correction. For model-1 and model-2, we collect 10 commonly used illuminants as test illuminants in open environment, the spectral power distribution of these illuminants are plotted in Figure 1, including tungsten halogen, fluorescent, F-series and LED illuminant. And the fluorescent illuminant in the 10 collected illuminants, with the correlation color temperature about 6500K, is selected as the reference illuminant (see the black line with asterisk in Figure 1). For model-3, an illuminant database including 701 illuminants that collected from different researches [15,16] is constructed for its testing, and the number of equivalent illuminants k is set to 20 according to the experiment experience.

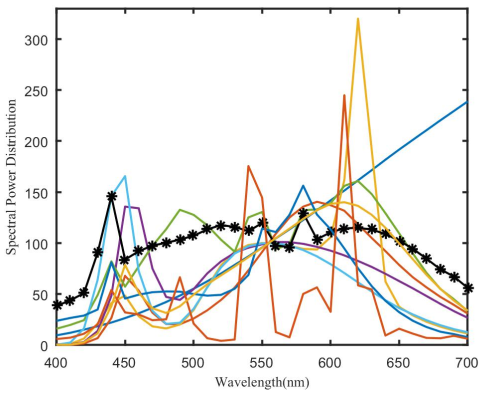

***Figure 1**. Spectral power distribution of the 10 collected illuminants*

Three sample sets including the X-rite ColorChecker charts, the Munsell colors and a group of mineral pigment samples are used in the experiment. The training set and testing set are listed in Table 1, and the numbers in brackets represent the number of samples of each set.

Table 1. Training and the corresponding testing samples

	Color chart	Munsell	Pigment
Training	SG (140)	odd (635)	odd (392)
Testing	CC (24)	even (634)	even (392)

The experimental result is evaluated in both spectral and colorimetric aspects. The root-mean-square error (*RMSE*) and the CIEL*a*b* color difference ΔE_{ab} are calculated between the estimated spectral and the ground-truth spectral. The methods to calculate *RMSE* and ΔE_{ab} are illustrated in equation (12) and equation (13), respectively.

$$RMSE = \sqrt{\frac{1}{\mathrm{N}}(\mathbf{r}_1 - \mathbf{r}_2)^T(\mathbf{r}_1 - \mathbf{r}_2)} \tag{12}$$

$$\Delta E_{ab} = \sqrt{(L_1^* - L_2^*)^2 + (a_1^* - a_2^*)^2 + (b_1^* - b_2^*)^2} \tag{13}$$

where $\mathbf{r}_1$ is the estimated spectral of the testing sample, $\mathbf{r}_2$ is the ground-truth spectral, the superscript T is the transpose operator, N is the sampling number of spectral in visible spectrum, for spectral wavelength ranges from 400 to 700nm at 10nm intervals, N=31. L^*, a^* and b^* are the colorimetric values of a sample in the CIELAB color space.

Result and Discussion

Using the above experimental conditions, the proposed method in three models of 'Model-1', 'Model-2' and 'Model-3' are tested. Table 2 and 3 summarize the average spectral estimation accuracy of the three sample sets and their overall average result. In addition, Figure 2 plots the average result of the three sample sets under 10 test illuminants for each model, so as to make a visual comparison of the performance of the three models. The abscissa numbers 1 to 10 in Figure 2 represent the 10 tested illuminant, respectively.

Table 2. The average spectral estimation error of *RMSE(%)* of the three sample sets and their overall average result

	Color chart	Munsell	Pigment	Average
Model-1	3.18	2.15	3.49	2.94
Model-2	2.74	1.90	3.25	2.63
Model-3	<u>2.58</u>	<u>1.78</u>	<u>3.07</u>	<u>2.48</u>

Table 3. The average spectral estimation error of ΔE_{ab} of the three sample sets and their overall average result

	Color chart	Munsell	Pigment	Average
Model-1	5.11	3.88	4.85	4.61
Model-2	4.01	2.92	3.68	3.54
Model-3	<u>3.51</u>	<u>2.38</u>	<u>3.06</u>	<u>2.98</u>

According to the statistics of the experimental results in Table 2 and 3, among the three testing models of the proposed method, no matter for a single sample set or for the average results of all the three sample sets, the 'Model-1' always shows the largest spectral estimation error, and the overall average error of the three experimental sample sets are 2.94 and 4.61 for *RMSE*(%) and ΔE_{ab}, respectively. The overall average spectral estimation error of 'Model-2' are 2.63 and 3.54 for *RMSE*(%) and ΔE_{ab}, and the overall spectral estimation average error of 'Model-3' are 2.48 and 2.98 for *RMSE*(%) and ΔE_{ab}.

Compare the three application models of the proposed method, the 'Model-2' and 'Model-3' show apparently better spectral estimation results than 'Model-1', which illustrate that the use of matrix $\mathbf{M}_1$ alone is not sufficient to achieve a better imaging condition correction result. On the basis of applying the matrix $\mathbf{M}_1$, the spectral estimation accuracy can be further improved by the further color correction. The result proved the importance of performing the further color correction to the object camera response. Besides, comparison of the results of 'Model-2' and 'Model-3' in Table 2 and 3 shows that both in terms of spectral and colorimetric accuracy, the 'Model-3' is always slightly better than the 'Model-2'. It is proved that to compare with the unified color correction matrix constructed by commonly used illuminants, the adaptive matrix constructed by estimated equivalent illuminants is more robust and superior for color correction applications.

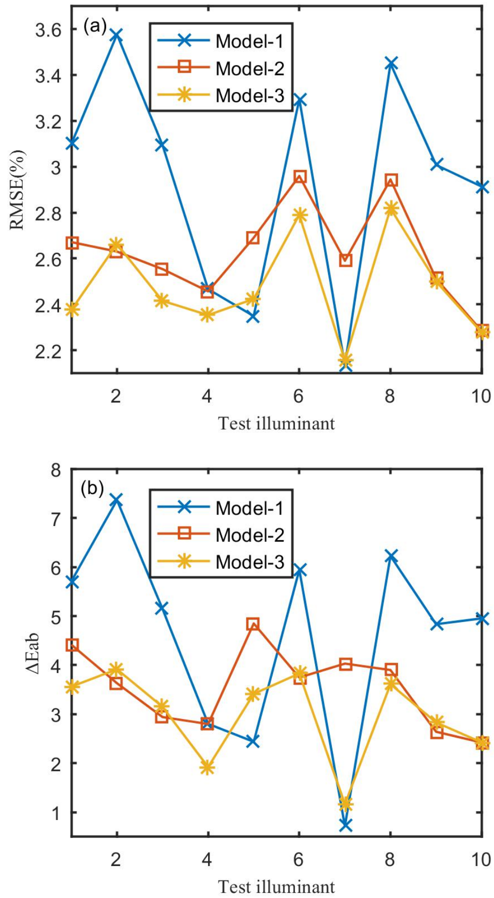

***Figure 2**. The average result of the three sample sets under 10 test illuminants for each model: (a) RMSE(%), (b) ΔE_{ab}*

In addition, it can be seen from Figure 2 that for the 10 tested illuminants, although the results of the three models showed some deviation from the above discussions under some illuminants, for most tested illuminants the distribution of the experimental results are consistent with the above discussion. In summary, the proposed spectral estimation method based on imaging condition correction in this study could theoretically realize the application of digital camera-based spectral estimation technology in open environment.

Conclusion

Digital camera-based spectral measurement technology has broad application prospects in many spectral-based analysis application fields. In order to resolve the problem that the current methods do not consider the exposure inconsistency between camera spectral characterization and spectral estimation applications in open environment, we proposed here a digital camera-based spectral estimation method based on imaging condition correction. The proposed method in three application models are tested through simulation experiment. Experimental results illustrate that the adaptive color correction model (the Model-3) in the proposed method for imaging condition correction shows the best spectral estimation accuracy, with the overall average *RMSE*(%) and ΔE_{ab} of 2.48 and 2.98. In the following studies, the practical application tests of the proposed method will be carried out in both outdoor and indoor unknown lighting environment.

References

[1] Yuqi Li, Chong Wang and Jieyu Zhao. Locally Linear Embedded Sparse Coding for Spectral Reconstruction From RGB Images. *IEEE Signal Processing Letters*, 25(3): 363-367, 2017.

[2] Taehoon Kim, Michelle A. Visbal-Onufrak, Raymond L. Konger and Young L. Kim. Data-driven imaging of tissue inflammation using RGB-based hyperspectral reconstruction toward personal monitoring of dermatologic health. *Biomedical Optics Express*, 8(11): 5282-5296, 2017.

[3] Bartosz Grabowski, Wojciech Masarczyk, Przemysław Głomb and Agata Mendys. Automatic pigment identification from hyperspectral data. *Journal of Cultural Heritage*, 31: 1-12, 2018.

[4] Alejandro Ribes and Francis Schmitt. Linear inverse problems in imaging. *IEEE Signal Processing Magazine*, 25(4): 84-99, 2008.

[5] Jinxing Liang and Xiaoxia Wan. Optimized method for spectral reflectance reconstruction from camera responses. *Optics Express*, 25(23): 28273-28287, 2017.

[6] Morteza M. Amiri and Mark D. Fairchild. Jones, A strategy toward spectral and colorimetric color reproduction using ordinary digital cameras. *Color Research and Application*, 43(5): 675-684, 2018.

[7] Jinxing Liang, Kaida Xiao, Michael R. Pointer, Xiaoxia Wan and Changjun Li. Spectra estimation from raw camera responses based on adaptive local-weighted linear regression. Optics Express 27(4): 5165-5180, 2019.

[8] Raju Shrestha and Jon Yngve Hardeberg. Spectrogenic imaging: A novel approach to multispectral imaging in an uncontrolled environment. *Optics Express*, 22(8): 9123-9133, 2014.

[9] Haris Ahmad Khan, Jean-Baptiste Thomas, Jon Yngve Hardeberg and Olivier Laligant. Spectral Adaptation Transform for Multispectral Constancy. J*ournal of Imaging Science and Technology*, 62(2):205041-2050412, 2018.

[10] Lijun Zhang, Jun Jiang, Hui Jiang, Jingjing Zhang and Xing Jin. Improving Training-based Reflectance Reconstruction via White-balance and Link Function, Proc. CCC, pg. 8616. (2018).

[11] Graham D. Finlayson, Michal Mackiewicz and Anya Hurlbert. Color Correction Using Root-Polynomial Regression. *IEEE Transactions on Image Processing*, 24(5): 1460-1470, 2015.

[12] Bin Cao, Ningfang Liao, Haobo Cheng. Spectral reflectance reconstruction from RGB images based on weighting smaller color difference group. *Color Research and Application*, 42(3): 327-332, 2017.

[13] Jueqin Qiu and Haisong Xu. Camera response prediction for various capture settings using the spectral sensitivity and crosstalk model. *Applied optics*, 55(25): 6989-6999, 2016.

[14] Maryam Mohammadzadeh Darrodi, Graham D. Finlayson, Teresa Goodman and Michal Mackiewicz. Reference data set for camera spectral sensitivity estimation. *JOSAA*, 32(3): 381-391, 2015.

[15] Kobus Barnard and Brian Funt.Camera Characterization for Color Research. *Color Research and Application*, 27(3): 152-163, 2002.

[16] Kevin W. Houser, Minchen Wei, Aurélien David, Michael R. Krames and Xiangyou Sharon Shen. Review of measures for light-source color rendition and considerations for a two-measure system for characterizing color rendition. *Optics Express*, 21(8): 10393-10411, 2013.

Author Biography

Dr. Jinxing Liang has received his M.Phil in Color and Imaging (2015) and PhD in Graphic Communication (2019) from Wuhan University in Wuhan, China. He was a visiting PhD student for one year at School of Design, University of Leeds, Leeds, UK. He is currently working as lecturer at College of Mathematics and Computer Science, Wuhan Textile University, Wuhan, China. He has (co-) authored more than 20 publications in the field of color and imaging science. His research interests include spectral imaging, color management and digital image processing. E-mail:jxliang@wtu,edu.cn.